Light-Fueled Microscopic Walkers

Hao Zeng, Piotr Wasylczyk, Camilla Parmeggiani, Daniele Martella, Matteo Burresi, and Diederik Sybolt Wiersma**

Nature provides a valuable source of inspiration for many fields of research. From optical effects to engineering problems, organisms have often adapted elaborate solutions and strategies, being the result of many years of natural selection.[1,2] Within this context, there is a lot of interest in creating artificial structures (robots) that can walk,[3] swim,[4] and perform various tasks.[5] Micrometer scale robots, in particular, have been proposed for applications, including drug delivery,[6] biosensing,[7] and microsurgery.[8] Based on the development of artificial muscles, a variety of soft robots that mimic natural creatures have been designed.[9–12] Such artificial creatures rely on power delivered from outside, while the entire mechanical actuation is due to the inner stress of the muscle. Differently from external field driven devices,[6,7] they approach naturally occurring living systems and are considered of broad scientific interest and technological value. Terrestrial soft robots have been realized with walking,[9,10] gripping,[11] and camouflage[12] functionalities, but still remain in the centimeter scale. Working in the microscopic scale, strong adhesion arising from the surface related forces (e.g., van der Waals and the capillary forces) is the limit of existing examples. Inspiringly, it has been found that in nature van der Waals and the capillary forces dominate the reversible adhesion between terrestrial living organisms and the surfaces in contact.[13–16] Typical natural adhesion force per unit area has been experimentally measured to be 0.3–1.3 MPa[17,18] (on gecko foot spatula), while a typical muscle stress in nature is between 0.01 and 0.2 MPa (peak 0.8 MPa).[19] While the entire creature size shrinks down to micrometers (muscle cross section getting close to body-environment contact area), the adhesion becomes comparable with the muscle force, thus posing a great difficulty for any movement. The balance between achievable muscle stress and adhesive forces thus sets the lower limit for the size of terrestrial free moving organisms, being of the order of 140 μm.[20] Similarly, microscopic artificial creatures equipped with artificial muscles are struggling to overcome the same adhesion hurdle as their natural relatives. The different physics ruling on microscopic length scales (including domination of adhesion forces) is worth exploring in micrometer-sized robotic systems. In addition, the realization of large numbers of autonomous robots can allow the study of cooperative effects, and open up new strategies for self-assembly.

Muscles (soft sections of the creatures) have always been well isolated from the environment, while hard crust and hairy-like surfaces often assist to reduce the surface contact zone and hence minimize the biological adhesion. Liquid crystalline elastomers (LCEs), that combine elastomeric properties with liquid crystalline orientational order, can reversibly deform in response to external stimuli with dramatic contraction (up to 400%) and with a stress compatible to natural muscles.[21] Therefore, LCEs have been considered as artificial muscles with great potential for creating biomimetic soft robot.[22] Recently developed technologies enable to control molecular order in the microscopic and macroscopic scale[23,24] (instinct related to actuation) and fabricate patterned actuator with micrometer-sized complex shapes.[25] However, such soft materials with typical elastic moduli $\boldsymbol{E}$ in the MPa range,[21] behave extremely sticky. All approaches to these artificial muscles in the microscopic scale have failed, as the natural adhesion poses a huge hurdle for robot's locomotion. To isolate the LCE muscle from the environment, and then solve the natural adhesion problem, we chose acrylic resin (IP-Dip) for fabrication of walker's limbs with a relative high $\boldsymbol{E}$ (≈4 GPa). The LCE composition shown in **Figure 1**a is chosen,[25] and interestingly the light sensitive element (azo-dye) is designed to open a transparency window for 780 nm fs laser and two-photon absorption polymerization at 390 nm in the direct laser writing (DLW) system, and to be activated by green light. DLW is used to pattern the complex 3D hybrid robot structures. This technique allows to arbitrary design 3D robot structures with nanometer scale resolution by a well control of sample position and laser exposure condition. Moreover, it consents a single polymerization/crosslinking step for the LC monomer mixture. Light energy is used to power the walker, with no external force applied. Approaching biological systems, such obtained artificial creatures are capable of different autonomous movements influenced by the interaction with their environment—similar to existing walking creatures in nature subject to the same van der Waals forces.

In the first stage, we prepared a LCE structure in order to characterize the optomechanical response of our materials, as reported in Figure 1. The mechanical response to light is fully reversible and consists in a contraction of around 20% along

Dr. H. Zeng, Prof. D. S. Wiersma
European Laboratory
for Non Linear Spectroscopy (LENS)
University of Florence
via Nello Carrara 1, 50019 Sesto, Fiorentino, Italy
E-mail: zeng@lens.unifi.it; wiersma@lens.unifi.it
Dr. P. Wasylczyk
LENS and Institute of Experimental Physics
Faculty of Physics
University of Warsaw
ul. Pasteura 5, 02-093 Warszawa, Poland
Dr. C. Parmeggiani, Dr. M. Burresi
LENS and Istituto Nazionale di Ottica (CNR-INO)
via Nello Carrara 1, 50019 Sesto, Fiorentino, Italy
Dr. D. Martella
LENS and Dipartimento di Chimica "Ugo Schiff"
University of Florence
via della Lastruccia 3-13, 50019 Sesto, Fiorentino, Italy

DOI: 10.1002/adma.201501446

© 2015 WILEY-VCH Verlag GmbH & Co. KGaA, Weinheim

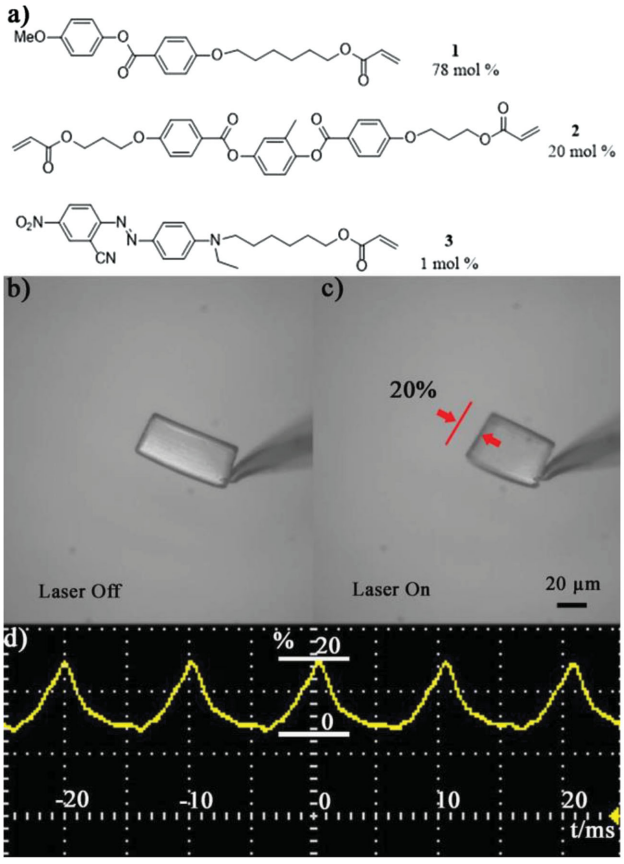

Figure 1. Liquid crystalline monomer composition and actuating response of a liquid crystalline elastomer (LCE) microstructure. a) Molecules used in the experiment. b) A $60 \times 30 \times 10$ μm^3 LCE actuator is held in the air on a glass tip. c) 20% contraction of the actuator along the long axis, while heated above 100 °C by a focused laser beam. d) Response of the same LCE structure under chopped 532 nm laser excitation at 100 Hz.

the director of the nematic liquid crystal elastomeric network (Figure 1b,c). For such specific elastomer it takes place via an intermediate heating step, which induces a phase transition (nematic–isotropic) in the material.[23] Illuminating the overall environment with light from a modulated, 532 nm laser source, the LCE responds following the laser modulation frequency (Figure 1d). High response frequency, 1.8 kHz, as shown in Figure S1d, Supporting Information, can be obtained. Such response is the fastest in the reported LCE muscles. The modulated amplitude decreases with increasing frequency (Figure S1, Supporting Information). Maximum light induced stress is measured to be 260 ± 2 kPa, which should be compared to natural muscles (10–200 kPa, and up to 1 kHz).[19,26] These parameters perfectly fit the needing for the microscopic robot construction.

In the fabrication process, an array of 3 μm high anchors were first fabricated on a polyimide (PI) coated, rubbed glass slide by DLW in IP-Dip (**Figure 2**a left). After removing the unsolidified resin (Figure 2a right), a 10 μm cell was formed by adding a PVA coated glass slide with parallel rubbing and infiltrated with the liquid-crystalline monomer mixture taking the nematic alignment along the rubbing.[25] The LCE actuator, being the $60 \times 30 \times 10$ μm^3 walker's main body, was made by DLW, with one side gripped by the anchors (Figure 2b). Subsequently, the lower glass slide is removed, and the whole structures are developed in toluene to remove the unsolidified LC monomers. Anchors (nonswelled in toluene) ensure proper adhesion between LCE (swelled in toluene) and the upper glass slide during development. In the last step the legs were made with the same technique as the anchors. The leg has a round, 12 μm diameter bottom, 0.5 μm top, and is 10 μm high (Figure 2c). Conical shape is chosen to reduce the surface contact area, while 45° tilt creates the adhesion asymmetry necessary for walking (SEM image in Figure 2d,e). Once the walker has been detached from the substrate, it is capable to perform reversible deformation under a modulated laser beam (Figure 2f and Movie S1, Supporting Information).

The artificial creature can automatically perform various locomotion highly depended on the interactions with the environment, which is demonstrated as follow. The walker was first set on a polyimide coated microscope glass slide surface. With the 532 nm laser beam chopped at 50 Hz, the body performs the contract-expand cycles following the laser modulation frequency. The light powered LCE actuator with 30×10 μm^2 cross section generates up to 78 μN force and the estimated total contact area of the leg pair is ≈0.4 μm^2 (inset in Figure 2e). Taking the maximum van der Waals attractive force[27] $F_{vdW} = A/6\pi D_0^3$ per unit area (Hamaker constant A is typically between[28] 0.5×10^{-19} and 1×10^{-19} J) and assuming that the gap between the leg and the glass is $D_0 = 0.3$ nm[27] and the friction coefficient μ being in the range from 0.2 to 1.0,[28] the maximum friction force $F = \mu F_{vdW}$ is between 7.9 and 78.5 μN. With the driving elastomeric force larger than the friction, the walker starts to slip. Local fluctuations of the adhesion on the nonuniform PI coating result in a random walking behavior—the instantaneous movement direction is determined by the friction differences from one leg to the other. An example of random walking trajectory is shown in **Figure 3**c (see Movie S2, Supporting Information). The friction strength on PI coating is relative high that the asymmetric tilted leg geometry does not provide any directional walking tendency. The walking velocity has an average value of some μms^{-1}, while the maximum speed is observed to be around 22 μm s^{-1}. In this mode, once a leg gets stuck to the surface, the walking terminates, and continuous rotation in one direction begins (Figure 3d–f, Movie S3, Supporting Information). The maximum rotation speed is measured in 1.5 rad s^{-1}.

In order to obtain directional walking on these length scales one has to overcome the local fluctuations in the adhesion forces. An example of this is reported in Figure 3g–i. The walker is positioned on a clean glass substrate and moves with a preferred direction defined by the leg tilt due to the shear off anisotropy, as previously demonstrated in biomimetic artificial adhesive structures.[29] No leg sticking is present; instead the continuous actuation of the walker body results in the net walking movement in the leg tilt direction. Local adhesion fluctuation may also induce rotation of the body, followed however by automatic reorientation (Figure 3i, Movie S4, Supporting Information). The walking direction is very sensitive to the friction fluctuation due to the small mass and to the high adhesion strength. Therefore, a straight walking direction is difficult to maintain. The average walking velocity in this case is measured to be around 37 μm s^{-1}.

© 2015 WILEY-VCH Verlag GmbH & Co. KGaA, Weinheim

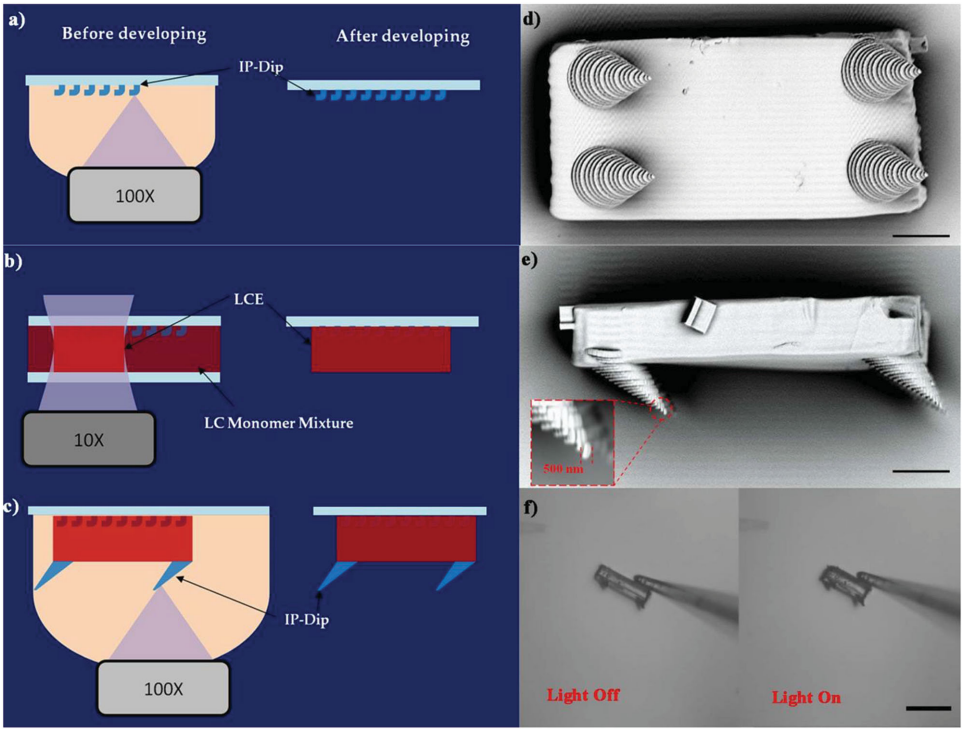

Figure 2. Fabrication of the microscopic walker. a) IP-Dip anchors were first fabricated on a rubbed polyimide coated glass by direct laser writing, followed by the developing process. b) A 10 μm gap cell was made by putting another PVA coated glass with parallel rubbing and infiltrated with the LC monomer mixture. The LCE body was made by the same laser writing system with a 10× microscope objective. c) Another drop of IP-Dip was applied, covering the fabricated structure and four conical legs were fabricated on the LCE body. d) SEM image of a microwalker lying upside down. Scale bar is 10 μm. e) Side view of the microwalker (scale bar: 10 μm), with 500 nm leg tip shown in the inset. f) Actuation of the microwalker under a 532 nm laser beam excitation (scale bar: 50 μm).

In the above case the walking direction is decided by the walker itself. It is also possible, on the other hand, to create an environment in which the direction is determined externally using patterned surfaces. On a blazed diffraction grating with 1300 lines per mm, the walker prefers to move in a certain direction, due to the interaction between different tilted nanoslope. A steady walking direction is maintained, independent from the leg tilt (Figure 3j–l)—the walker can actually rotate the full 360° while maintaining the net movement direction (Movie S5, Supporting Information). On such grating surface, a 10 times larger walking velocity (380 μm s^{-1}) comparing to the previous cases has been observed.

Yet another behavior—up to ≈1 cm (100 body lengths) long jumps—was obtained on a Teflon surface. Conical legs provide advantage for walking, however, they can easily get stuck into the micro-gully on the Teflon surface. For this reason, we have also designed the walker with a 100 × 50 × 10 μm^3 body size and three sets of lamellar legs (see Figure S2, Supporting Information). By increasing the laser power, such robot approached to the maximum deformation and stored the light energy inside the LCE body as elastic potential. At some point the walker overcome the adhesion on one side, and the elastic body converted the elastic energy into kinetic energy. Thus, a sudden jump occurred as shown in Movie S6 in the Supporting Information. Inspired by fleas,[30] jumping could be a more efficient way of transport for robots at the micrometer scale, where the influence of gravity and inertia are significantly reduced and the air drag dominates the kinetic energy loss (see the Experimental Section).

In conclusion, we demonstrated the preparation of a microscopic walker entirely powered by light and based on LCE artificial muscles. The locomotion of such artificial creatures is influenced by their design and how they interact with the environment—random or directional walking, rotation or jumping is possible and demonstrated above. With an average muscle stress of 200 kPa, assuming 1 μm^2 of the foot-surface contact area and taking adhesive forces per unit area of 1 MPa into account, a minimum muscle cross section of 5 μm^2 is needed to overcome adhesion for every single step. This results in the lower estimate of moving terrestrial creatures of the order of tens of micrometers, already saturated by our walker. Note that, although a laser source was used for convenience in all the experiments, such laser is defocused and illuminates large areas and the LCE muscles can, in principle, use energy from any light source. Importantly, there is also no need to target specific individual parts of the robots with a light beam. The walkers simply absorb the light from their overall environment. Optimization of the body geometry, actuator shape, and action and the leg tilt angle may still result in improved locomotion performance. The method presented allows to create, in principle, large amounts of elastomer-based robots in a relatively easy manner and with a versatile approach. Variety of LCE-based autonomous robot can be expected, e.g., microswimmers, microjumpers, origami photonic devices, and so on.

© 2015 WILEY-VCH Verlag GmbH & Co. KGaA, Weinheim

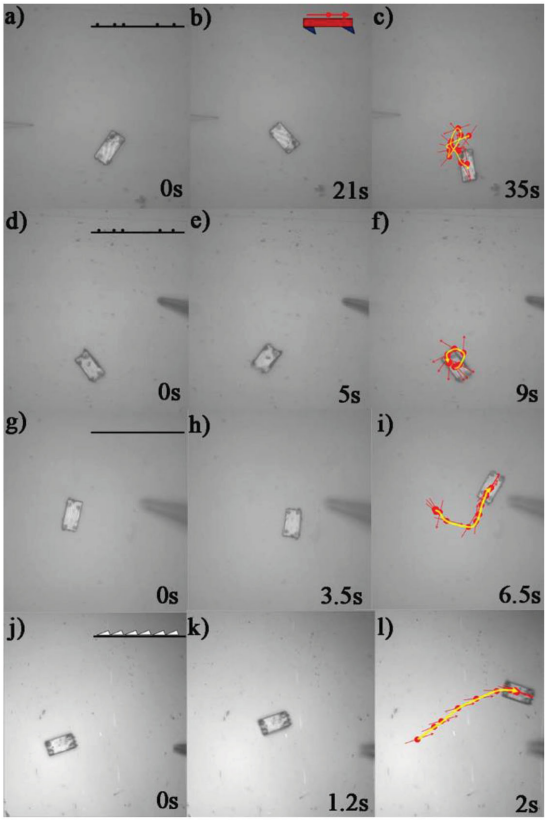

Figure 3. Surface dependent locomotion behaviors. Under the same chopped laser excitation (532 nm, 50 Hz, 10 W mm^{-2}), the 60 μm size microscopic walker: a–c) randomly walks on the PI coated glass surface; d–f) rotates with one leg stuck onto the PI coated surface; g–i) walks with self-reorientation on the clean glass surface; j–l) walks in the direction determined by the grating groove pattern (vertical). Insets of (a), (d), (g), (j) show the schematics of the surface. Inset in (b) shows the orientation of the arrow with respect to the walker.

Experimental Section

Materials: The monomer mixture contains 78 mol% of the LC monomer **1**, 20 mol% of the LC crosslinker **2**, 1 mol% of the azo dye **3**, and 1 mol% of the photoinitiator (Irgacure 369) as reported by Zeng et al.[25]

Direct Laser Writing Fabrication: Fabrication of the walker was peformed in a Dip-in Laser Lithography system (Nanoscribe GmbH). Sample preparation and development followed the procedure presented in ref. [25].

Characterization: For testing the LCE light response, a $60 \times 30 \times 10$ μm^3 LCE actuator was held on a glass tip. Two laser beams: 300 mW continuous 532 nm solid state laser and 2 mW He-Ne laser were focused on the center and edge of the structure, respectively, by a 20× (NA 0.4) objective. The 532 nm laser was chopped to induce the modulated deformation, while the transmitted He-Ne laser beam was detected by a photodiode as a signal related to the LCE deformation.

Two glass tips (1 and 5 μm in diameter) were used to transfer the microwalker onto different substrates with the help of 3D manual translation stages. A chopped 532 nm laser was defocused by a 10× objective (NA = 0.2) to a spot of around 200 μm diameter and ≈10 W mm^2 intensity for the walker actuation. As the walker body temperature exceeded 100 °C under laser illumination the environment could be assumed to be dry, and thus ignored capillary interactions. A scanning electron microscope (PHENOM-World) was used to observe the structures after sputter-coating them with a 10 nm gold layer.

Light-Induced Stress Measurement: For measuring the light induced stress, a $5 \times 2.5 \times 0.05$ mm^3 LCE sample was hung vetically attached to a force sensor and a 532 nm laser illumination (5 W cm^{-2}) was applied to induce contraction. A maximum stress of 260 ± 2 kPa was measured.

Glass Treatment: The surface of the glass substrates was cleaned by rinsing in a 1:300 diluted HF water solution for 10 min.

Jumping Dynamics Estimation: Assuming 50% of the elastic energy turned into kinetic energy the launch speed was ≈4.7 ms^{-1} (LCE Young's modulus $E \approx 1.3$ MPa, density $\rho_{LCE} = 1.16$ g cm^{-3}, and strain of 20%). The Reynolds number *Re* was calculated to be no more than 12 ($Re = \rho v D/\mu$, air density $\rho = 1.2$ kg m^{-3}, velocity $v < 4.7$ ms^{-1}, approximate object diameter $D = 40$ μm, air dynamic viscosity $\mu = 18.6$ μPa s) for the entire flight. In a low Reynolds number environment, the drag contributed to the majority of the energy lost.

Supporting Information

Supporting Information is available from the Wiley Online Library or from the author.

Acknowledgments

The research leading to these results has received funding from the IIT SEED project Microswim and the European Research Council under the European Union's Seventh Framework Programme (FP7/2007–2013)/ ERC Grant Agreement No. 291349 on photonic microrobotics. H.Z. was supported by the ICTP Ph.D. Program. The authors gratefully thank the entire Optics of Complex Systems group at LENS for feedback and discussions.

Received: March 26, 2015
Revised: April 26, 2015
Published online: May 28, 2015

[1] K. Liu, L. Jiang, *Nano Today* **2011**, *6*, 155.
[2] B. Bhushan, *Philos. Trans. R. Soc. A* **2009**, *367*, 1445.
[3] M. Rubenstein, A. Cornejo, R. Nagpal, *Science* **2014**, *15*, 795.
[4] A. J. Ijspeert, A. Crespi, D. Ryczko, J.-M. Cabelguen, *Science* **2007**, *315*, 1416.
[5] R. Pfeifer, M. Lungarella, F. Iida, *Science* **2007**, *318*, 1088.
[6] S. Kim, F. Qiu, S. Kim, A. Ghanbari, C. Moon, L. Zhang, B. J. Nelson, H. Choi, *Adv. Mater.* **2013**, *25*, 5863.
[7] F. Qiua, R. Mhanna, L. Zhang, Y. Ding, S. Fujita, B. J. Nelson, *Sens. Actuators, B* **2014**, *196*, 676.
[8] R. A. Freitas, *Int. J. Surg.* **2005**, *3*, 243.
[9] R. F. Shepherd, F. Ilievski, W. Choi, Stephen A. Morin, A. A. Stokes, A. D. Mazzeo, X. Chen, M. Wang, G. M. Whitesides, *Proc. Natl. Acad. Sci. USA* **2011**, *108*, 20400.
[10] M. Moua, R. R. Kohlmeyer, J. Chen, *Angew. Chem. Int. Ed.* **2013**, *52*, 9234.
[11] R. F. Shepherd, A. A. Stokes, R. M. D. Nunes, G. M. Whitesides, *Adv. Mater.* **2013**, *25*, 6709.
[12] S. A. Morin, R. F. Shepherd, S. W. Kwok, Adam A. Stokes, A. Nemiroski, G. M. Whitesides, *Science* **2012**, *337*, 828.
[13] K. Autumn, M. Sitti, Y. A. Liang, A. M. Peattie, W. R. Hansen, S. Sponberg, T. W. Kenny, R. Fearing, J. N. Israelachvili, R. J. Full, *Proc. Natl. Acad. Sci. USA* **2002**, *99*, 12252.
[14] A. B. Kesel, A. Martin, T. Seidl, *Smart Mater. Struct.* **2004**, *13*, 512.
[15] W. Federle, E. L. Brainerd, T. A. McMahon, B. Holldobler, *Proc. Natl. Acad. Sci. USA* **2001**, *98*, 6215.
[16] G. Huber, H. Mantz, R. Spolenak, K. Mecke, K. Jacobs, S. N. Gorb, E. Arzt, *Proc. Natl. Acad. Sci. USA* **2005**, *102*, 16293.

© 2015 WILEY-VCH Verlag GmbH & Co. KGaA, Weinheim

[17] H. Lee, B. P. Lee, P. B. Messersmith, *Nature* **2007**, *448*, 338.
[18] G. Huber, S. N. Gorb, R. Spolenak, E. Arzt, *Biol. Lett.* **2005**, *1*, 2.
[19] R. J. Full, K. Meijer, *Natural Muscles as an Electromechanical System. Electroactive Polymer (EAP) Actuators as Artificial Muscles—Reality, Potential and Challenges* (Ed. Y. Bar-Cohen), SPIE Press, Bellingham, WA, **2001**, pp. 67–83.
[20] E. L. Mockford, *Ann. Entomol. Soc. Am.* **1997**, *90*, 115.
[21] C. Ohm, M. Brehmer, R. Zentel, *Adv. Mater.* **2010**, *22*, 3366.
[22] M. Yamada, M. Kondo, R. Miyasato, Y. Naka, J. Mamiya, M. Kinoshita, A. Shishido, Y. Yu, C. J. Barrett, T. Ikeda, *J. Mater. Chem.* **2009**, *19*, 60.
[23] H. Zeng, P. Wasylczyk, G. Cerretti, D. Martella, C. Parmeggiani, D. S Wiersma, *Appl. Phys. Lett.* **2015**, *106*, 111902.
[24] T. H. Ware, M. E. McConney, J. Jae Wie, V. P. Tondiglia, T. J. White, *Science* **2015**, *347*, 982.
[25] H. Zeng, D. Martella, P. Wasylczyk, G. Cerretti, J.-C. G. Lavocat, C.-H. Ho, C. Parmeggiani, D. S. Wiersma, *Adv. Mater.* **2014**, *26*, 2319.
[26] D. S. Smith, *J. Biophys. Biochem.Cytol.* **1961**, *10*, 123.
[27] Y. Tian, N. Pesika, H. Zeng, K. Rosenberg, B. Zhao, P. McGuiggan, K. Autumn, J. Israelachvili, *Proc. Natl. Acad. Sci. USA* **2006**, *103*, 19320.
[28] D. Leckband, J. Israelachvili, *Q. Rev. Biophys.* **2001**, *34*, 105.
[29] M. P. Murphy, B. Aksak, M. Sitti, *Small* **2009**, *5*, 170.
[30] G. P. Sutton, M. Burrows, *J. Exp. Biol.* **2011**, *214*, 836.

© 2015 WILEY-VCH Verlag GmbH & Co. KGaA, Weinheim